




 Cite this: *RSC Adv.*, 2018, 8, 35681

New nano-Fe₃O₄-supported Lewis acidic ionic liquid as a highly effective and recyclable catalyst for the preparation of benzoxanthenes and pyrroles under solvent-free sonication†

 Hai Truong Nguyen,  Ngoc-Phuong Thi Le, Duy-Khiem Nguyen Chau and Phuong Hoang Tran *

A novel magnetic nanomaterial-immobilized Lewis acidic ionic liquid was successfully synthesized by the covalent embedding of 3-(3-(trimethoxysilyl)propyl)-1*H*-imidazol-3-ium chlorozincate (ii) ionic liquid to the surface of Fe₃O₄ nanoparticles. The material was then characterized by FT-IR, SEM, TEM, TGA, ICP-OES, Raman, and EDS. Its performance as a new-generation Lewis acidic catalyst was also examined on the ultrasound-mediated synthesis of benzoxanthenes and pyrroles. Upon completion, the catalyst was simply recovered by an external magnet for multiple reuses without significant lessening of catalytic performance.

 Received 7th June 2018
Accepted 10th October 2018

DOI: 10.1039/c8ra04893b

rsc.li/rsc-advances

Introduction

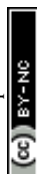
Owing to their exceptional physical and chemical properties, ionic liquids (ILs) have gained increasing application as green solvents/catalysts for various organic transformations.^{1–4} Among them, Lewis acidic ionic liquids (LAILs) have been intensively studied as efficient alternatives for traditional Lewis acidic catalysts in many organic syntheses to facilitate higher yielding transformation to wanted products within short reaction times.^{5–8} Despite the mentioned preeminence, these LAILs still have several drawbacks such as the elaborate procedure for catalyst recovery and product isolation as well as the demand for the excessive amount of ILs in biphasic systems, which in turn would raise concerns about economical and toxicological issues.^{9,10} As a result, various solid-supported ionic liquids have been progressively developed to overcome those challenges thanks to their capability of being handled, separated, and recycled with ease.^{11–19} Recently, our group successfully employed a Brønsted acidic ionic liquid gel as a heterogeneous catalyst to assist the preparation of bisindolylmethanes.¹⁹ Despite the outstanding recyclability, low yields were inevitable because of the poor dispersion of the ionic liquid gel in the reaction mixture. Being aware of this shortcoming, relevant scientific communities are continuously directing their attention to employ high-surface-area materials as new-generation catalyst supports for multiple organic reactions. Among them,

magnetic nanoparticles have been extensively studied on a variety of principal organic transformations including C–C, C–N, and C–O coupling since their magnetism can enable a much simplified work-up procedure where nanoparticle-supported catalysts are promptly separated from the reaction media by an external permanent magnet rather than filtration and centrifugation.^{12,13,20,21} However, in contrast to the widespread availability of organocatalysts impregnated on solid supports, the preparation of solid-immobilized ionic liquids has been still a great challenge. To the best of our knowledge, there have been only a few reports on the use of magnetic material-supported ionic liquids in some organic reactions.^{12,15–17,22–29} Many of them are the impregnated forms of Brønsted acidic ionic liquids. Therefore, the demand for designing new magnetic nanoparticle-supported Lewis acidic ionic liquids has still remained a topical interest since various organic transformations can be promoted by Lewis acidic species.

Based on the above fundamental understandings, we reported herein the designation of a novel magnetic nanoparticle-immobilized Lewis acidic ionic liquid and its usage as a prominent catalyst for the preparation of benzoxanthenes and pyrroles, two important heterocyclic scaffolds commonly present in various bioactive natural products, agrochemicals, and pharmaceuticals.^{30–44} Although a large number of catalytic procedures have been developed for quantitative synthesis of these heterocycles, the attempt of searching for a versatile catalyst fulfilling all green chemistry criteria, such as high-turnover property, excellent recyclability, simplicity in handling and recycling, and the capacity of promoting reactions under mild condition, has been still an unsolved problem. The initial results from our screening effort to find novel ionic

Department of Organic Chemistry, Faculty of Chemistry, University of Science, Viet Nam National University, Ho Chi Minh City 721337, Vietnam. E-mail: thphuong@hcmus.edu.vn

† Electronic supplementary information (ESI) available. See DOI: 10.1039/c8ra04893b



liquid-based catalysts for certain organic reactions indicated that magnetic nanomaterial Fe_3O_4 -supported Lewis acidic ionic liquid could be the best candidate most likely satisfying all mentioned requirements. Its outstanding catalytic performance over the multicomponent synthesis of benzoxanthenes and Paal-Knorr condensation to prepare pyrroles in this paper promises its prospectively common use as a novel catalyst in replacement of conventional Lewis acidic ones in organic synthesis. As far as we have known, this is the first report on the synthesis and catalytic reactivity of a magnetic nanoparticle-immobilized Lewis acidic ionic liquid.

Results and discussion

Characterization of LAIL@MNP

The magnetic nano- Fe_3O_4 -immobilized Lewis acidic ionic liquid material (LAIL@MNP) was prepared in accordance to the protocol presented in Scheme 1. Initially, magnetite ferrite nanoparticle was formed *via* a co-precipitation method while the precursor ionic liquid was independently synthesized by the treatment of (3-chloropropyl)triethoxysilane with imidazole. Then the outermost surface of MNP was coated with the prepared ionic liquid. Finally, ZnCl_2 was added and the resulting mixture was heated under reflux for 24 h to afford LAIL@MNP.

The grafting of LAIL@MNP was verified by FT-IR analysis. Fig. 1b and c showed the IR spectra of primitively synthesized LAIL@MNP and its recycled sample after the fifth recycling test, respectively. As expected, a good resemblance between two spectra can be seen over a wide range of absorption band, including peaks at 3430 cm^{-1} (broad absorption corresponding to Si-OH group and adsorbed water), 2921 cm^{-1} (aliphatic C-H stretch), 1620 cm^{-1} ($\text{C}=\text{N}$ stretch of imidazolium ring), and a cluster of two peaks at 1095 and 1043 cm^{-1} (Si-O-Si stretch). These signals were not observed in the spectrum of plain Fe_3O_4 (Fig. 1a). This indicated that ionic liquid was successfully grafted onto the surface of the Fe_3O_4 nanoparticle.

Scanning electron microscopy (SEM) image in Fig. 2 showed the morphology of LAIL@MNP which is depicted as uniform spherical particles. Transmission electron microscopy (TEM) confirmed that dark Fe_3O_4 core coated by grey silica shell has the average diameter of 10–15 nm (Fig. 2).

The thermostability of the LAIL@MNP was studied by thermogravimetric analysis (TGA) (Fig. 3). The TGA curve indicates an initial weight loss of 0.74% in the temperature range below 200°C , most likely corresponding to the evaporation of residual water from the sample. The entire loss of the grafted LAIL was detected in the region from 220°C to 400°C . The percentage of

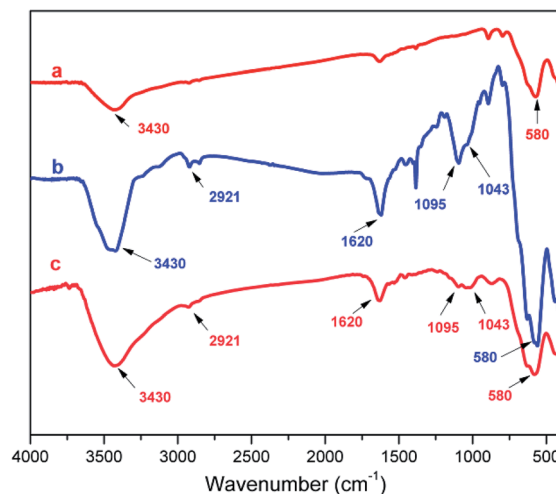


Fig. 1 FT-IR spectra of Fe_3O_4 (a), primitively prepared LAIL@MNP (b), and the LAIL@MNP sample after the fifth recovery (c).

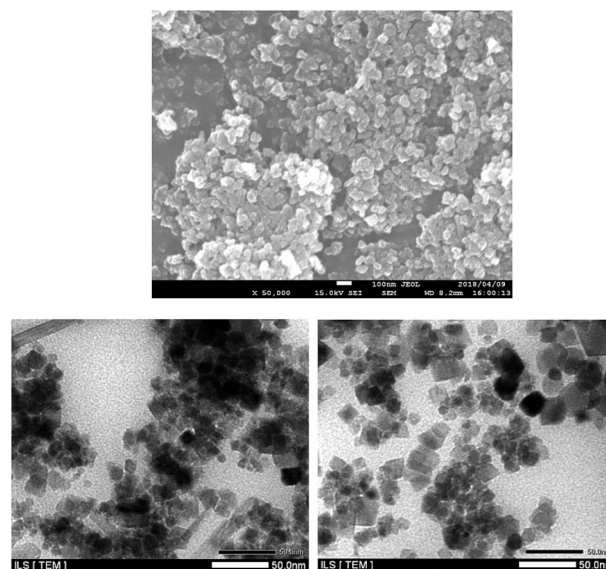
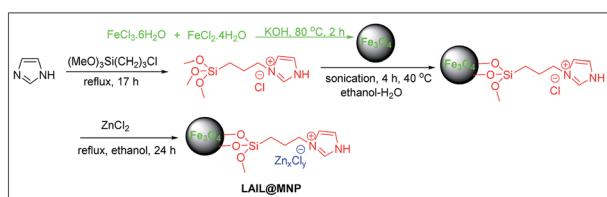


Fig. 2 SEM image of LAIL@MNP (above) and TEM images (below) of as-prepared (left) and quinary recycled LAIL@MNP (right).

LAIL, as determined, was approximately 3% of the total solid matrix. The Raman peak at 480 cm^{-1} can be interpreted as stretching vibration of Zn-Cl bond.⁴⁵ The energy dispersive spectrum (EDS) showed the presence of C, N, O, Fe, Zn, Si, and



Scheme 1 Synthesis of LAIL@MNP.

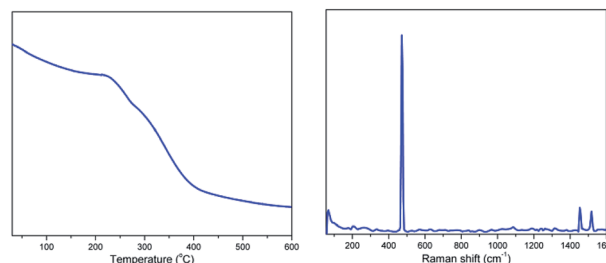


Fig. 3 TGA curve of LAIL@MNP (left) and its Raman spectrum (right).



Cl elements (Fig. 4). The composition of zinc element in LAIL@Fe₃O₄ was determined as 19 890 ppm (0.306 mmol g⁻¹) by means of inductively coupled plasma mass spectrometry (ICP-MS).

Synthesis of benzoxanthene derivatives

Initially, the catalytic activity of LAIL@MNP was surveyed in an ultrasound-assisted solvent-free multicomponent synthesis of pyran-annulated heterocyclic derivatives from 2-naphthol, dimedone, and benzaldehyde. As can be seen from Table S1,† significantly prolonged exposure to ultrasound (120 min) was necessitated for a quantitative formation of desired product (94%) at room temperature (entry 11). As expected, performing the reaction at an elevated temperature of 80 °C can bring the reaction to completion within 30 min (entry 18). Noticeably, the extremely poor yield of benzoxanthene was observed in control experiment where no catalyst was used (entry 23). Surprisingly, the addition of 1 mg of LAIL@MNP to the reaction mixture can give rise to a tremendous enhancement of reaction yield from 10% to 65% (entry 24). The transformation of given starting materials to the expected product can be brought to completion by increasing the catalyst loading from 1 to 15 mg (Table S1,† entry 18 and 24).

Subsequently, to illustrate the merit of LAIL@MNP, a variety of other catalysts were also studied for their activity with respect to the same reaction for the comparative purpose (Table S2†). In general, the investigated multicomponent reaction seems likely

to be favored in acidic media as all metal halides, which are known as typical Lewis acids, can effectively furnish the benzoxanthene product in good yields of at least 80% (entry 5–9). Analogously, an array of different ionic liquids possessing weakly Brønsted acidic imidazolium species can also readily facilitate the formation of the same annulated product without any difficulty (entry 1–4). Meanwhile, most of the metal oxides, because of their predominant Lewis basicity, only exhibited moderate catalytic performance under the given reaction condition (entry 10–19). The invention of LAIL@MNP material having Lewis acidic zinc species immobilized onto magnetic Fe₃O₄ nanoparticle not only brought about a remarkable yield increment but also enable a quite simple work-up step for product isolation as well as catalyst recovery (entry 21). The effect of solvent on the studied reaction was also investigated, showing that low yield of product was observed with polar as well as nonpolar solvents (Table S2,† entries 22–36).

As can be seen from Table 1, the current method gave access to the desired product with the same ease as those reported in the literature. However, LAIL@MNP still gained prominence over other heterocyclic catalysts owing to its capability to enable the reaction under solventless condition. Additionally, the affordability of ZnCl₂ also makes the protocol described herein more advantageous than the others of using expensive transition-metal catalysts.

With the optimized condition in hand, we then examined the performance of catalyst over a wide range of aldehydes. As indicated in Scheme 2, the reaction generally worked well for saturated aliphatic as well as aromatic aldehydes. On the contrary, α,β -unsaturated aldehydes such as acrolein and cinnamaldehyde almost did not undergo the annulation with 2-naphthol and dimedone even under prolonged reaction time due to the positive charge delocalization arising from resonance effect. As expected, butyraldehyde with less steric hindrance at α -position was more reactive than cyclohexanecarbaldehyde. Under the same condition, 78% yield of the benzoxanthene derived from butyraldehyde was recorded, compared to the yield of 65% noted for the analogue produced from cyclohexanecarbaldehyde. Surprisingly, all benzaldehydes bearing either electron-donating or electron-withdrawing groups afforded the corresponding products from good to excellent yields (70–90%). Interestingly, steric hindrance of bulky *o*-substituents such as bromo or nitro in aromatic aldehydes did not bring about any detectable negative impact on the reaction as reported above for aliphatic aldehydes. The structural study of

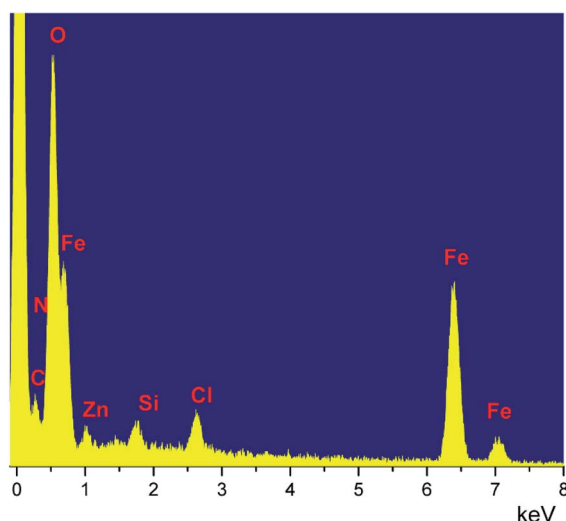
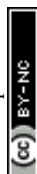
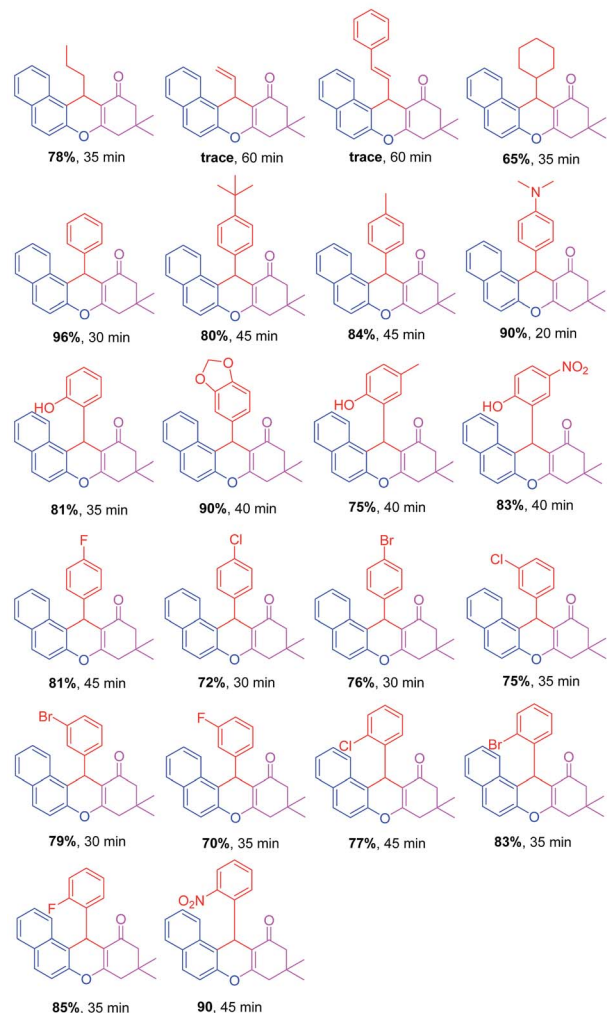
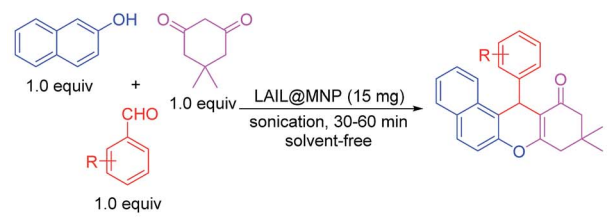


Fig. 4 EDS spectrum of LAIL@MNP.

Table 1 Comparative effectiveness of the current method *versus* former works for the three-component synthesis of benzoxanthenes

Entry	Catalytic system	Temp. (°C)	Time (h)	Yield (%)
1	Nano Fe ₃ O ₄ /CS-Ag (15 mg)	80	0.5	94 (ref. 46)
2	Ru@SH-MWCNT (15% wt), EtOH/reflux	80	0.5	85 (ref. 47)
3	Nano-WO ₃ -SO ₃ H (19 mg)	100	1.05	90 (ref. 48)
4	W-ZnO (5.6 mol%), EtOH	r.t.	0.17	98 (ref. 49)
5	Amberlyst-15 (200 mg), CH ₃ CN	Reflux	5	94 (ref. 50)
6	AIL@MNP (55 mg), dimedone (2.0 equiv.)	90	0.75	89 (ref. 24)
7	Current work: LAIL@MNP (15 mg), solvent-free sonication	80	0.5	96

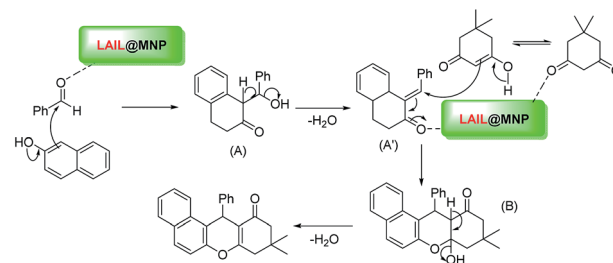




Scheme 2 Reaction scope of the three-component condensation of 2-naphthol, dimedone, and aldehyde in the presence of $\text{Fe}_3\text{O}_4@\text{SiO}_2\text{-IL-ZnX}_2$.

benzoxanthenes by X-ray crystallography in the previous literature revealed that the phenyl half is orthogonal rather than coplanar to the other half to minimize the steric strain of the whole molecule.⁵¹ Therefore, the steric effect of *o*-substituents in phenyl moiety is negligible owing to the flat structure of benzene ring. However, this is not the case for an aliphatic half like cyclohexyl since its uneven configuration always causes inevitable steric interaction regardless of its spatial arrangement in the molecule.

Based on the current results and previous literature,^{32,36,52,53} a proposed mechanistic profile for the synthesis of benzoxanthenes using LAIL@MNP is depicted in Scheme 3. According



Scheme 3 Proposed mechanism for one-pot multicomponent synthesis of benzoxanthenes.

to this mechanism, the coordination between zinc species and carbonyl oxygen enhances the electrophilicity of carbonyl carbon, giving rise to a better nucleophilic attack of 2-naphthol to benzaldehyde to furnish α,β -unsaturated cyclic ketone intermediate (A') after the loss of water molecule. Then Michael addition between this intermediate and the enol form of dimedone followed by the dehydration afforded the expected product.

Synthesis of pyrrole

The Paal-Knorr synthesis of 2,5-dimethyl-1-phenyl-1*H*-pyrrole from aniline and acetylacetone was chosen as the second example to examine the catalytic performance of LAIL@MNP and the results are listed in Table S3.[†] In the presence of 15 mg of LAIL@MNP, the reaction proceeded smoothly to provide the expected pyrrole in quantitative yield of 91% after 30 min of sonication.

To exemplify the novelty of LAIL@MNP, the same reaction was probed over a wide range of catalysts and the results are presented in Table S4.[†] Similar to the above discussed multicomponent reaction, Paal-Knorr condensation has been also known to take place in slightly acidic rather than basic media. Consequently, all metal halides with Lewis acidic properties can straightforwardly bring the yield of pyrrole to more than 80% (entry 4–8), while metal oxides with amphoteric or basic nature only resulted in poor to moderate formation of the desired pyrrole under the same condition (entry 9–18). Without a rival, LAIL@MNP was again proven as the best candidate to induce a complete transformation to the target pyrrole (entry 20).

The comparison of the present method with formerly reported works was summarized in Table 2. Most obviously, the fact that LAIL@MNP promoted the synthesis of pyrrole under solvent-free condition can be easily outlined as the most noteworthy advantage compared with existing catalysts.

The tolerance of the presently studied Paal-Knorr reaction towards different functionalities was described in Scheme 4. In general, the reaction was apparently governed by both electronic and steric effect. Therefore, *p*-substituted anilines bearing an electron-donating (–OMe) or a weakly electron-withdrawing group (–I) can most easily undergo Paal-Knorr cyclization to offer corresponding products in quantitative yields more than 90%. Meanwhile, the analog containing strongly electron-withdrawing group, *p*-nitroaniline, can be only converted to the desired pyrrole with a quite modest yield of



Table 2 Comparison of the present synthesis of pyrrole with previous works in literature

Entry	Catalyst	Temp. ^a (°C)	Time (h)	Yield ^b (%)
1	Bi(NO ₃) ₃ · 5H ₂ O (50 mol%), CH ₂ Cl ₂	r.t.	10	95 (ref. 54)
2	I ₂ (0.1 mmol), THF	r.t.	9	89 (ref. 55)
3	Sc(OTf) ₃ (5 mol%), CH ₂ Cl ₂	r.t.	0.5	77 (ref. 56)
4	In(OTf) ₃ (5 mol%), CH ₂ Cl ₂	r.t.	0.5	90 (ref. 57)
5	[BMIm]Cl	r.t.	3	96 (ref. 58)
6	SbCl ₃ /SiO ₂ (0.1 mmol), hexane	r.t.	1	91 (ref. 59)
7	BiCl ₃ /SiO ₂ (7.5 mmol), hexane	r.t.	1	92 (ref. 60)
8	Vitamin B1 (5 mol%), ethanol	r.t.	1	90 (ref. 61)
9	α-Zr(KPO ₄) ₂ (6 mol%)	r.t.	2	78 (ref. 62)
10	Montmorillonite, KSF (1 g), CH ₂ Cl ₂	r.t.	10	95 (ref. 63)
11	PS/AlCl ₃ (15 mol%), CH ₃ CN	Reflux	1.25	90 (ref. 64)
12	This work: LAIL@MNP, solvent-free sonication	r.t.	0.5	91

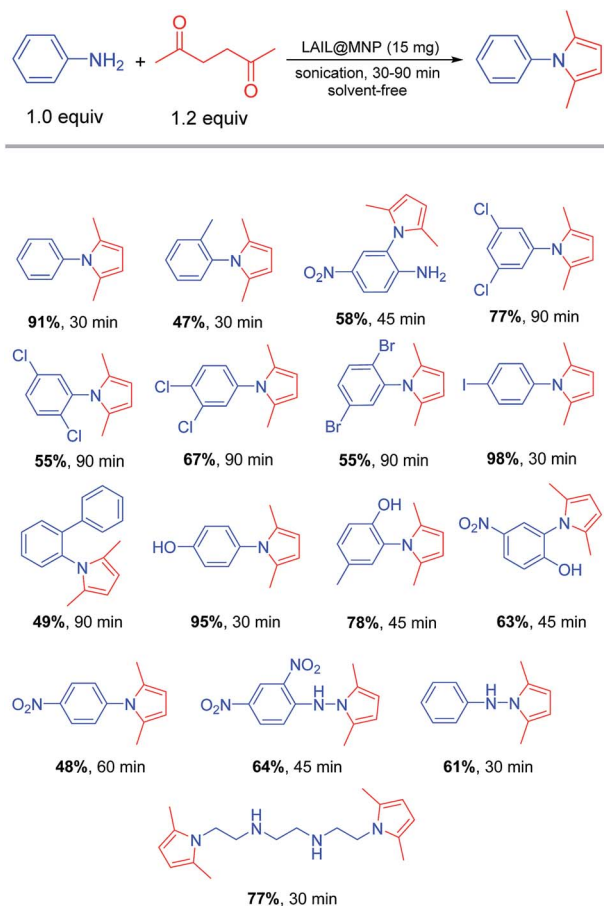
^a r.t.: room temperature. ^b Isolated yield.

48% even though the reaction time was extended up to 60 min. Shifting the methoxy group to *ortho*-position with respect to reactive amino site resulted in a diminished yield. The dominance of steric effect can be unambiguously observed for all *o*-substituted anilines bearing bulky groups, such as methyl, chloro, bromo, and phenyl. For instance, the pyrrole derived from 2,5-dichloroaniline was formed in much lower yield than those generated from 3,4- and 3,5-dichloroaniline isomers. Noticeably, regardless of its small size, *o*-methoxy group was

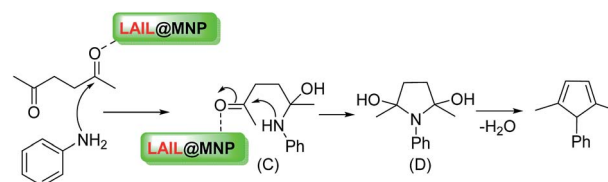
also able to exhibit a certain steric effect suppressing the complete transformation to desired products wherein pyrroles derived from 2-hydroxy-5-methylaniline and 2-hydroxy-5-nitroaniline were isolated in 78 and 63% yield, respectively. Interestingly, selective pyrrole cyclization can be achieved thanks to the directing effect of present substituents. As illustrated in Scheme 4, only the amino group at *meta*-position to nitro substituent was exclusively subjected to the Paal-Knorr condensation with acetonylacetone while the other was intact. Finally, the extension of substrate scope to phenylhydrazines and triethylenetetramine was also applicable for this method.

A proposed mechanism for the formation of pyrrole catalyzed by LAIL@MNP is depicted in Scheme 5. In a similar fashion to the above mechanism for the multicomponent synthesis of benzoxanthene, carbonyl oxygen of acetonylacetone is first coordinated to zinc center to generate a better electrophilic species which more readily reacts with amine to give intermediate adduct (C). Following intramolecular nucleophilic cyclization with the loss of two molecules of water delivers the desired pyrrole.

The recyclability of LAIL@MNP was examined over both benzoxanthene and pyrrole synthesis under the reported optimized condition (Fig. 5). Upon the completion of each reaction, the corresponding product was diluted with ethyl acetate (15 mL) and the catalyst was separated by a magnet. The restored catalyst was washed with ethyl acetate (2 × 5 mL) and ethanol (3 × 5 mL). Then it was desiccated *in vacuo* for 2 h and reutilized in the next recycling experiments. Nearly quantitative LAIL@MNP could be recovered from each run. The stability and efficacy of LAIL@MNP remained constant through five consecutive recycling tests. No apparent modification in morphology and size of particles was detected in the TEM image of primitively prepared



Scheme 4 Synthesis of pyrrole derivatives.



Scheme 5 A plausible mechanism for the synthesis of pyrroles.



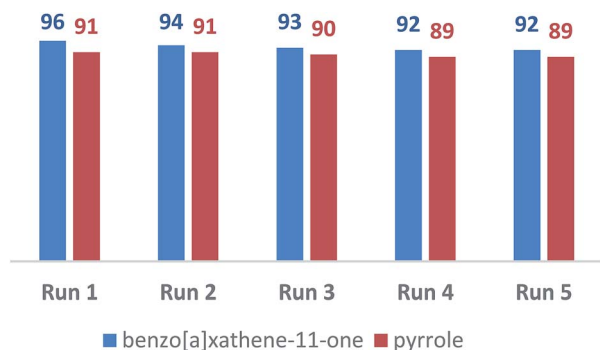


Fig. 5 Recycling tests.

as well as recovered sample of LAIL@MNP (Fig. 2). The FT-IR spectra of LAIL@MNP samples also suggested no obvious change in functionality (Fig. 1).

The primary issue of heterogeneous catalysts is the leaching of reactive species from solid support, resulting in deactivation of the catalyst. To evaluate the leaching effect of LAIL@MNP, the reaction between aniline and acetonylacetone was temporarily stopped after 10 min by diluting the ongoing reaction mixture with a sufficient amount of ethyl acetate. The catalyst was then removed and the ethyl acetate solution was analyzed by GC, indicating that 58% yield of pyrrole was formed at that time. Next, ethyl acetate solvent was decanted and the resultant free-catalyst reaction mixture was sonicated for further 20 min. At the end of this stage, the yield of pyrrole only slightly increased from 58 to 62%, showing that only a trace amount of zinc species was leached into the reaction mixture during the reaction course. The leaching level of LAIL@MNP was also evaluated by ICP-OES whereby the Zn content in reaction mixture was determined as 1.8 ppm, indicating a negligibly slight leaching from the solid support.

Experimental

Preparation of magnetic Fe₃O₄ nanoparticle (MNPs)⁶⁵

MNP was synthesized by simple co-precipitation of ferrous and ferric ions in a basic condition medium. Typically, FeCl₃·6H₂O (20 mmol) and FeSO₄·7H₂O (10 mmol) were dissolved in 100 mL deionized water. The mixture was stirred at 80 °C and then KOH (12 mmol) was added and stirred continuously within 2 h. The black precipitate, after being collected by a permanent magnet, was washed with water (3 × 100 mL) and ethanol (3 × 50 mL). This MNP material was dried at 60–70 °C under *vacuo* for 1 h.

General procedure for the synthesis of LAIL@MNP

The imidazolium chloride ionic liquid was synthesized pursuant to a procedure reported previously.⁶⁶ A mixture of 3-chloroethoxy-propylsilane (5.0 mmol, 1.2 mL) and imidazole (5.0 mmol, 0.34 g) was stirred at reflux for 17 h. The ionic liquid obtained as a yellowish viscous liquid was diluted in 50 mL of ethanol–water (1 : 1 volume ratio) solution. To the freshly prepared suspension of MNP material in 100 mL of 1 : 1 ethanol–water was added the above ionic liquid solution and

the mixture was sonicated at 40 °C for 4 h. The resultant IL@MNP was washed with dichloromethane and dried at 70 °C *in vacuo*. To synthesize LAIL@MNP, a mixture of IL@MNP (1.0 g) and ZnCl₂ (1.0 mmol) in ethanol (50 mL) was refluxed for 24 h. After cooling to room temperature, the catalyst was separated by a magnet, washed with ethanol, and dried at 100 °C for 5 h. The LAIL@MNP was characterized by FT-IR, SEM, TEM, TGA, Raman, and SEM-EDS. The loading amount of Zn metal was determined based on ICP-OES.

General procedure for one-pot multicomponent reaction

A mixture of benzaldehyde (1.0 mmol, 0.106 g), 2-naphthol (1.0 mmol, 0.144 g), and dimedone (1.0 mmol, 0.140 g) was reacted under solvent-free sonication in the presence of LAIL@MNP (15 mg) at 80 °C for 30 min. Upon completion of the reaction (monitored by TLC), the resulting mixture was diluted by ethyl acetate (15 mL) and the solid catalyst was eliminated from organic solution by a magnet. The catalyst was washed with ethyl acetate (2 × 5 mL) followed by ethanol (3 × 5 mL) and then reused for next cycles after drying under vacuum. Meanwhile, the organic solution was dried over MgSO₄ and then concentrated under reduced pressure. The resultant crude product was recrystallized from ethanol to yield pure benzoxanthene whose structure was verified by ¹H and ¹³C NMR.

General procedure for Paal–Knorr reaction

A mixture of aniline (1.0 mmol), acetonylacetone (1.2 mmol) and LAIL@MNP (15 mg) was reacted under solvent-free sonication within an appropriate interval. Upon completion of the reaction (monitored by TLC and GC), the resulting mixture was diluted by ethyl acetate (15 mL) and the solid catalyst was eliminated from the organic solution by a magnet. The catalyst was washed with ethyl acetate (2 × 5 mL) followed by ethanol (3 × 5 mL) and then reused for next cycles after drying under vacuum. Meanwhile, the organic solution was dried over MgSO₄ and then concentrated under reduced pressure. The crude product was purified through column chromatography using hexane–ethyl acetate (9 : 1). The purified pyrrole was then authenticated by ¹H and ¹³C NMR, GC-MS or HRMS (ESI).

Conclusions

We have designed a novel magnetically separable LAIL@MNP material which can be used as a green solid Lewis acid catalyst in various organic reactions. Embedding reactive Lewis acidic sites onto high-surface area Fe₃O₄ nanomaterial greatly overcame the issue of poor dispersion which is common for heterogeneous catalysts. Owing to this feature, LAIL@MNP can exhibit better catalytic performance than conventional Lewis acid in acid-mediated organic reactions such as multicomponent and Paal–Knorr reactions to synthesize benzoxanthenes and pyrroles, respectively, in good to excellent yields. Additionally, the efficiency of the protocol was also owing to the use of ultrasonic irradiation by means of which locally high collapse temperature induced by the successive formation and collapse of cavitation bubbles in reaction media can extraordinarily



enhance the reaction rate. Moreover, the catalyst was easily separated from the reaction mixture by an external magnetic field and reused without any significant loss of catalytic activity after five runs.

Conflicts of interest

There are no conflicts to declare.

Acknowledgements

This project is financially supported by Vietnam National Foundation for Science and Technology Development (NAFOS-TED) through research grant 104.01-2016.59.

Notes and references

- M. A. Martins, C. P. Frizzo, A. Z. Tier, D. N. Moreira, N. Zanatta and H. G. Bonacorso, *Chem. Rev.*, 2014, **114**, PR1-PR70.
- Q. Wang, W. Hou, S. Li, J. Xie, J. Li, Y. Zhou and J. Wang, *Green Chem.*, 2017, **19**, 3820-3830.
- K. Goossens, K. Lava, C. W. Bielawski and K. Binnemans, *Chem. Rev.*, 2016, **116**, 4643-4807.
- D. J. Kim, K. H. Oh and J. K. Park, *Green Chem.*, 2014, **16**, 4098-4101.
- A. S. Amarasekara, *Chem. Rev.*, 2016, **116**, 6133-6183.
- H. T. Nguyen and P. H. Tran, *RSC Adv.*, 2016, **6**, 98365-98368.
- X. Zhang, R. Zhang, X. Meng, H. Liu, Z. Liu, H. Ma, C. Xu and P. A. A. Klusener, *Appl. Catal., A*, 2018, **557**, 64-71.
- F. Abbasi, N. Azizi and M. Abdoli-Senejani, *Appl. Organomet. Chem.*, 2017, **31**, 3790-3796.
- H. Niedermeyer, J. P. Hallett, I. J. Villar-Garcia, P. A. Hunt and T. Welton, *Chem. Soc. Rev.*, 2012, **41**, 7780-7802.
- J. P. Hallett and T. Welton, *Chem. Rev.*, 2011, **111**, 3508-3576.
- P. C. Marr and A. C. Marr, *Green Chem.*, 2016, **18**, 105-128.
- A. Pourjavadi, S. H. Hosseini, M. Doulabi, S. M. Fakoorpoor and F. Seidi, *ACS Catal.*, 2012, **2**, 1259-1266.
- R. K. Sharma, S. Dutta, S. Sharma, R. Zboril, R. S. Varma and M. B. Gawande, *Green Chem.*, 2016, **18**, 3184-3209.
- J. D. Patil, S. A. Patil and D. M. Pore, *RSC Adv.*, 2015, **5**, 21396-21404.
- N. Azgomi and M. Mokhtary, *J. Mol. Catal. A: Chem.*, 2015, **398**, 58-64.
- H. N. Dadhania, D. K. Raval and A. N. Dadhania, *Catal. Sci. Technol.*, 2015, **5**, 4806-4812.
- X. Liang, *Ind. Eng. Chem. Res.*, 2014, **53**, 17325-17332.
- Y.-M. Wang, V. Ulrich, G. F. Donnelly, F. Lorenzini, A. C. Marr and P. C. Marr, *ACS Sustainable Chem. Eng.*, 2015, **3**, 792-796.
- P. H. Tran, X.-T. T. Nguyen and D.-K. N. Chau, *Asian J. Org. Chem.*, 2018, **7**, 232-239.
- B. Zhen, Q. Jiao, Y. Zhang, Q. Wu and H. Li, *Appl. Catal., A*, 2012, **445-446**, 239-245.
- Y. Kong, R. Tan, L. Zhao and D. Yin, *Green Chem.*, 2013, **15**, 2422-2433.
- Y. Zhang and C. Xia, *Appl. Catal., A*, 2009, **366**, 141-147.
- J. Miao, H. Wan and G. Guan, *Catal. Commun.*, 2011, **12**, 353-356.
- Q. Zhang, H. Su, J. Luo and Y. Wei, *Green Chem.*, 2012, **14**, 201-208.
- B. Karimi, F. Mansouri and H. Vali, *Green Chem.*, 2014, **16**, 2587-2596.
- P.-H. Li, B.-L. Li, H.-C. Hu, X.-N. Zhao and Z.-H. Zhang, *Catal. Commun.*, 2014, **46**, 118-122.
- Z. Wu, Z. Li, G. Wu, L. Wang, S. Lu, L. Wang, H. Wan and G. Guan, *Ind. Eng. Chem. Res.*, 2014, **53**, 3040-3046.
- H. N. Dadhania, D. K. Raval and A. N. Dadhania, *Res. Chem. Intermed.*, 2017, **44**, 117-134.
- Q. Zhang, X.-M. Ma, H.-X. Wei, X. Zhao and J. Luo, *RSC Adv.*, 2017, **7**, 53861-53870.
- J. Safaei-Ghomi and F. Eshteghal, *Ultrason. Sonochem.*, 2017, **38**, 488-495.
- N. Azizi and F. Shirdel, *J. Mol. Liq.*, 2016, **222**, 783-787.
- F. Taghavi, M. Gholizadeh, A. S. Saljooghi and M. Ramezani, *RSC Adv.*, 2016, **6**, 87082-87087.
- A. R. Moosavi-Zare, M. A. Zolfigol, O. Khaledian, V. Khakyzadeh, M. D. Farahani, M. H. Beyzavi and H. G. Kruger, *Chem. Eng. J.*, 2014, **248**, 122-127.
- A. R. Moosavi-Zare, M. A. Zolfigol, M. Zarei, A. Zare and V. Khakyzadeh, *J. Mol. Liq.*, 2013, **186**, 63-69.
- J. M. Khurana and D. Magoo, *Tetrahedron Lett.*, 2009, **50**, 4777-4780.
- G. C. Nandi, S. Samai, R. Kumar and M. S. Singh, *Tetrahedron*, 2009, **65**, 7129-7134.
- A. Kornienko and J. J. La Clair, *Nat. Prod. Rep.*, 2017, **34**, 1051-1060.
- M. Fleige and F. Glorius, *Chem.-Eur. J.*, 2017, **23**, 10773-10776.
- F. Bonyasi, M. Hekmati and H. Veisi, *J. Colloid Interface Sci.*, 2017, **496**, 177-187.
- A. Kamal, S. Faazil, M. Shaheer Malik, M. Balakrishna, S. Bajee, M. R. H. Siddiqui and A. Alarifi, *Arabian J. Chem.*, 2016, **9**, 542-549.
- L. Zhang, J. Zhang, J. Ma, D.-J. Cheng and B. Tan, *J. Am. Chem. Soc.*, 2017, **139**, 1714-1717.
- J. Sączewski, J. Fedorowicz, M. Gdaniec, P. Wiśniewska, E. Sieniawska, Z. Dražba, J. Rzewnicka and Ł. Balewski, *J. Org. Chem.*, 2017, **82**, 9737-9743.
- Z. Gong, Y. Lei, P. Zhou and Z. Zhang, *New J. Chem.*, 2017, **41**, 10613-10618.
- H. Truong Nguyen, D.-K. Nguyen Chau and P. H. Tran, *New J. Chem.*, 2017, **41**, 12481-12489.
- H. Pir, N. Günay, Ö. Tamer, D. Avcı, E. Tarcan and Y. Atalay, *Mater. Sci.-Pol.*, 2013, **31**, 357-371.
- E. E. Reza Mohammadi, M. Ghavami and M. Z. Kassaei, *J. Mol. Catal. A: Chem.*, 2014, **393**, 309-316.
- K. Tabatabaeian, M. A. Zanjanchi, M. Mamaghani and A. Dadashi, *Res. Chem. Intermed.*, 2016, **42**, 5049-5067.
- S. R. Ali Amoozadeh, *J. Mol. Catal. A: Chem.*, 2015, **396**, 96-107.
- F. S. Arbosara, F. Shirini, M. Abedini and H. F. Moafi, *J. Nanostruct. Chem.*, 2015, **5**, 55-63.



- 50 B. Das, B. Ravikanth, R. Ramu, K. Laxminarayana and B. V. Rao, *J. Mol. Catal. A: Chem.*, 2006, **255**, 74–77.
- 51 K. Aggarwal and J. M. Khurana, *J. Mol. Struct.*, 2015, **1079**, 21–34.
- 52 X. J. Sun, J. F. Zhou and P. S. Zhao, *J. Heterocycl. Chem.*, 2011, **48**, 1347–1350.
- 53 V. Rama, K. Kanagaraj and K. Pitchumani, *Tetrahedron Lett.*, 2012, **53**, 1018–1024.
- 54 B. K. Banik, I. Banik, M. Renteria and S. K. Dasgupta, *Tetrahedron Lett.*, 2006, **46**, 2643–2645.
- 55 R. H. Peiris, C. Hallé, H. Budman, C. Moresoli, S. Peldszus, P. M. Huck and R. L. Legge, *Water Res.*, 2010, **44**, 185–194.
- 56 J. Chen, H. Wu, Z. Zheng, C. Jin, X. Zhang and W. Su, *Tetrahedron Lett.*, 2006, **47**, 5383–5387.
- 57 A. Rahmatpour, *J. Organomet. Chem.*, 2012, **712**, 15–19.
- 58 B. Wang, Y. Gu, C. Luo, T. Yang, L. Yang and J. Suo, *Tetrahedron Lett.*, 2004, **45**, 3417–3419.
- 59 M. R. P. Hossein Reza Darabi, K. Aghapoor, A. Mirzaee, F. Mohsenzadeh, N. Asadollahnejad, H. Taherzadeh and Y. Balavar, *Environ. Chem. Lett.*, 2012, **10**, 5–12.
- 60 K. Aghapoor, L. Ebadi-Nia, F. Mohsenzadeh, M. Mohebi Morad, Y. Balavar and H. R. Darabi, *J. Organomet. Chem.*, 2012, **708–709**, 25–30.
- 61 K. A. Hossein Reza Darabi and F. M. Abbas Darestani Farahani, *Environ. Chem. Lett.*, 2012, **10**, 369–375.
- 62 M. Curini, F. Montanari, O. Rosati, E. Lioy and R. Margarita, *Tetrahedron Lett.*, 2003, **44**, 3923–3925.
- 63 B. K. Banik, S. Samajdar and I. Banik, *J. Org. Chem.*, 2004, **69**, 213–216.
- 64 A. Rahmatpour and J. Aalaie, *Heteroat. Chem.*, 2011, **22**, 85–90.
- 65 J. Safari and Z. Zarnegar, *C. R. Chim.*, 2013, **16**, 920–928.
- 66 S. Nazari, S. Saadat, P. K. Fard, M. Gorjizadeh, E. R. Nezhad and M. Afshari, *Monatsh. Chem.*, 2013, **144**, 1877–1882.

